Research Article Vol. 33, No. 2 / 27 Jan 2025 / Optics Express 1827
Optics EXPRESS

Diffraction-free partially coherent Pearcey beam

TIANYU CAO,[1,2,3] SHENGTAI JIN,[1,2,3] QIAN CHEN,[1,2,3] PUJUAN MA,[1,2,3,6] SERGEY A. PONOMARENKO,[4,5] YANGJIAN CAI,[1,2,3,7] CHUNHAO LIANG,[1,2,3,8] AND JINGSONG LIU[1,2,3,9]

[1]*Shandong Provincial Engineering and Technical Center of Light Manipulations & Shandong Provincial Key Laboratory of Optics and Photonic Device, School of Physics and Electronics, Shandong Normal University, Jinan 250014, China*
[2]*Collaborative Innovation Center of Light Manipulations and Applications, Shandong Normal University, Jinan 250358, China*
[3]*Joint Research Center of Light Manipulation Science and Photonic Integrated Chip of East China Normal University and Shandong Normal University, East China Normal University, Shanghai 200241, China*
[4]*Department of Electrical and Computer Engineering, Dalhousie University, Halifax, Nova Scotia B3J 2X4, Canada*
[5]*Department of Physics and Atmospheric Science, Dalhousie University, Halifax, Nova Scotia B3H 4R2, Canada*
[6]*pujuanma@foxmail.com*
[7]*yangjiancai@sdnu.edu.cn*
[8]*chunhaoliang@sdnu.edu.cn*
[9]*liujs@sdnu.edu.cn*

Abstract: Partially coherent beams are renowned for their inherent resilience against environmental perturbations. However, traditional versions are prone to distortion due to light diffraction, which presents significant challenges for related applications such as information transfer. In this paper, we theoretically and experimentally construct a non-diffraction, partially coherent Pearcey beam. The results clearly demonstrate such a beam remains invariant during propagation under different coherence conditions. The experimental results align closely with the theoretical predictions. We believe that this beam has the potential to offer new insights as an information carrier for optical communication and information transmission, particularly in adverse environments.

© 2025 Optica Publishing Group under the terms of the Optica Open Access Publishing Agreement

1. Introduction

Partially coherent beams (PCBs) have the stable statistical properties, even though they allow for fluctuations in both phase and intensity across the beam and over time [1]. Their inherent ability to suppress beam interference and then reduce optical noise ensures reliable performance in speckle-free optical imaging, super-resolution optical holography, and high-performance photonic computing applications [2–5]. Further, based on optical coherence theory, PCBs can be considered an incoherent superposition of multiple modes [1]. These beams are renowned for their inherent resilience to environmental perturbations, as the perturbative effects on individual modes tend to cancel each other out [6]. This characteristic makes PCBs particularly well-suited for crucial applications such as optical communications, far-field optical imaging, and optical encryption and decryption in adverse environments [7–10]. In recent years, the degree of coherence, as a unique degree of freedom of PCBs, has triggered extensive research activity from the fundamental physics to valuable applications [11–24]. Notably, the degree of coherence has been explored as an information carrier for image encryption [10,16], and by introducing randomness, PCBs have achieved high-capacity information encryption [9]. However, PCBs with low coherence are susceptible to optical diffraction, leading to the deterioration of all degrees of freedom, including the degree of coherence, during propagation. As a result, the encrypted

#545959 https://doi.org/10.1364/OE.545959
Journal © 2025 Received 24 Oct 2024; revised 6 Dec 2024; accepted 21 Dec 2024; published 13 Jan 2025

Optics EXPRESS

information is inevitably compromised. The basic idea to overcome this challenge lies in the construction of partially coherent diffraction-free beams.

On the other hand, diffraction-free beams, as the exact solutions of the homogeneous Helmholtz equation [25], remain their shape unchanged during propagation in free space. Since the pioneering work of Durnin et al. [25,26], these beams have garnered significant interest. According to Babinet's Principle, all such beams are naturally immune to the distortions [7,27]. They have found a variety of applications in volumetric imaging [28], ghost imaging [29], particle trapping [30], photon correlation holography [31], and prime number factorization [14]. Partially coherent diffraction-free beams receive growing attention due to the inborn advantages of both PCBs and diffraction-free beams. To date, two main methods have been proposed to realize these beams. First, Turunen et al. obtained partially coherent solutions by solving the coupled Helmholtz equations, revealing that the key property of such beams lies in the "incoherence" of the angular correlation function of their plane-wave components in the radial direction, while the correlation in the azimuthal direction can be arbitrary [32]. It provides valuable insight into the effects of varying the degree of coherence, and demonstrates a Bessel-correlated source is one example of partially coherent diffraction-free beams. Second, partially coherent diffraction-free beams can be customized via the incoherent superposition of fully coherent diffraction-free modes.Incoherent superposition refers to the combination of fields that have no fixed phase relationship with each other. Through adopting different coherent modes as well as their weight coefficient, various types of beams have emerged, such as dark and anti-dark beam, Airy beams on incoherent background, partially coherent diffraction-free vortex beams [27,33–35].

In this paper, we follow the incoherent superposition principle to construct partially coherent diffraction-free Pearcey beam. The primary distinction between our work and the traditional partially coherent self-accelerating beams lies in the mode selection [36–38]. We chose the eigenmode of an incoherent system - the cosine mode - while they utilized the eigenmode of a coherent system. Consequently, after incoherent superposition, the partially coherent Pearcey beams we constructed keep invariant during propagation in free space.

2. Theoretical model and analysis

In space-frequency domain, the statistical properties of the PCBs are characterized by the cross-spectrum density (CSD) function. It reads as follows:

$$W(\mathbf{r}_1, \mathbf{r}_2) = \int p(\mathbf{k}) A^*(\mathbf{k}, \mathbf{r}_1) A(\mathbf{k}, \mathbf{r}_2) d^2\mathbf{k}, \tag{1}$$

where $p(\mathbf{k})$ represents the power spectrum density function, and $A(\mathbf{k}, \mathbf{r})$ is any kernel function. $\mathbf{r} = (x, y)$ and $\mathbf{k} = (k_\perp, k_\parallel)$ are the vector positions in the source plane and reciprocal plane, respectively. Different from the traditional fully coherent Pearcey beam [39,40], to construct non-diffracting partially coherent Pearcey beams, we adopt the following form

$$p(\mathbf{k}) = \frac{{\sigma_c}^2}{2\pi} \exp\left(-\frac{1}{2}\mathbf{k}^2\sigma_c^2\right), \tag{2}$$

$$A(\mathbf{k}, \mathbf{r}) = \cos\left(\frac{1}{2}\sigma_I^4 k_\perp^4 + \frac{1}{2}\sigma_I^4 k_\parallel^4 + \frac{1}{2}k_\perp x + \frac{1}{2}k_\parallel y\right), \tag{3}$$

where σ_c and σ_I stand for the coherence width and beam width, respectively. Here we introduce the dimensionless sum and difference coordinates as

$$\mathbf{R}_+ = (\mathrm{X}_+, \mathrm{Y}_+) = (\mathbf{r}_1 + \mathbf{r}_2)/2\sigma_I, \mathbf{R}_- = (\mathrm{X}_-, \mathrm{Y}_-) = (\mathbf{r}_1 - \mathbf{r}_2)/\sigma_I. \tag{4}$$

On substituting from Eqs. (2)-(4) into Eq. (1), the CSD function of the desired beam can be rewritten as follows:

$$W(\mathbf{R}_+, \mathbf{R}_-) = W_b(\mathbf{R}_+) + W_g(\mathbf{R}_-), \tag{5}$$

Optics EXPRESS

where

$$W_b(\mathbf{R}_+) = \frac{q_I^c}{4\pi}\mathrm{Re}\left[\mathrm{Pe}\left(\mathrm{X}_+, iq_I^c/2\right)\mathrm{Pe}\left(\mathrm{Y}_+, iq_I^c/2\right)\right], \tag{6}$$

$$W_g(\mathbf{R}_-) = \exp\left(-\mathbf{R}_-^2 \Big/ 8q_I^c\right), \tag{7}$$

where $\mathrm{Pe}(\cdot,\cdot)$ is a Pearcey function, defined by $\mathrm{Pe}(a,b) = \int_{-\infty}^{+\infty}\exp\left[i\left(s^4 + as^2 + bs\right)\right]ds$, and $q_I^c = \sigma_c^2/\sigma_I^2$ determines the global coherence of the source beam. The CSD function depends on only one parameter q_I^c . $W_b(\mathbf{r}_+)$ is a bump function atop the background, with the latter being characterized by $W_g(\mathbf{r}_-)$. The propagation behavior of the PCBs can be studied with the help of the Fresnel diffraction integral [1], as follows:

$$\begin{aligned} W(\boldsymbol{\rho}_1, \boldsymbol{\rho}_2) = \iint W(\mathbf{r}_1, \mathbf{r}_2)\exp\left[-\frac{ik}{2z}\left(\mathbf{r}_1^2 - 2\mathbf{r}_1\cdot\boldsymbol{\rho}_1 + \boldsymbol{\rho}_1^2\right)\right] \\ \exp\left[\frac{ik}{2z}\left(\mathbf{r}_2^2 - 2\mathbf{r}_2\cdot\boldsymbol{\rho}_2 + \boldsymbol{\rho}_2^2\right)\right]d^2\mathbf{r}_1 d^2\mathbf{r}_2. \end{aligned} \tag{8}$$

By substituting from Eqs. (5–7) into Eq. (8) and converting to dimensionless sum and difference coordinates, after straightforward integration, we demonstrate that the CSD function of the diffraction-free partially coherent Pearcey beam remains independent of the propagation distance z, i.e., $W(\mathbf{R}_+, \mathbf{R}_-, z) = W(\mathbf{R}_+, \mathbf{R}_-, z = 0)$. This clearly proves such a beam is immune to optical diffraction.

However, this beam exhibits an infinite profile, symbolizing boundless energy, which is not physically realizable. To address this, we introduce a Gaussian aperture as a truncation function for the beam. The CSD function of the truncated version is then rewritten by $W_p(\mathbf{R}_+, \mathbf{R}_-) = \exp\left(-\alpha^2\mathbf{R}_+^2 - \alpha^2\mathbf{R}_-^2/4\right) \times W_i(\mathbf{R}_+, \mathbf{R}_-)$, where $\alpha = \sigma_I/\sigma_0$ and σ_0 denotes the width of the truncation function. To further explore the beam properties of the truncated diffraction-free partially coherent Pearcey beam, and facilitate its experimental construction, we employ the pseudo-mode superposition principle [27] to represent such beam,

$$W_p(\mathbf{r}_1, \mathbf{r}_2) = \sum_{m,n} p(\mathbf{k}_{mn}) A_p^*(\mathbf{k}_{mn}, \mathbf{r}_1) A_p(\mathbf{k}_{mn}, \mathbf{r}_2), \tag{9}$$

where $p(\mathbf{k}_{mn})$ is a discretized power spectrum density function and here characterizes the mode weight. $A_p(\mathbf{k}_{mn}, \mathbf{r}_2)$ is the truncated mode (or pseudo-mode), defined by

$$A_p(\mathbf{k}_{mn}, \mathbf{r}) = \exp\left(-\frac{\mathbf{r}^2}{2\sigma_0^2}\right)A(\mathbf{k}_{mn}, \mathbf{r}). \tag{10}$$

Here $\mathbf{k}_{mn} = (m \times d, n \times d)$, $m, n \in [0, N]$ denotes the location of sampling point in the reciprocal plane, where d is sampling space and N is total number of sampling points along horizontal or vertical direction. Since free space is a linear system, the propagation behavior of truncated diffraction-free partially coherent Pearcey beams can be evaluated through the incoherent superposition of all pseudo-modes propagating to the receiver plane, with the help of optical wave propagation theory [1].

3. Results and analysis

In this section, we investigate the beam properties using the aforementioned equations and numerical simulations. The intensity and degree of coherence distributions of the beam at the source are displayed in the left and right panels of Fig. 1, respectively. The coherent width σ_c is set as σ_c = 1mm. As the value of the global coherencen q_I^c decreases, the main central

Optics EXPRESS

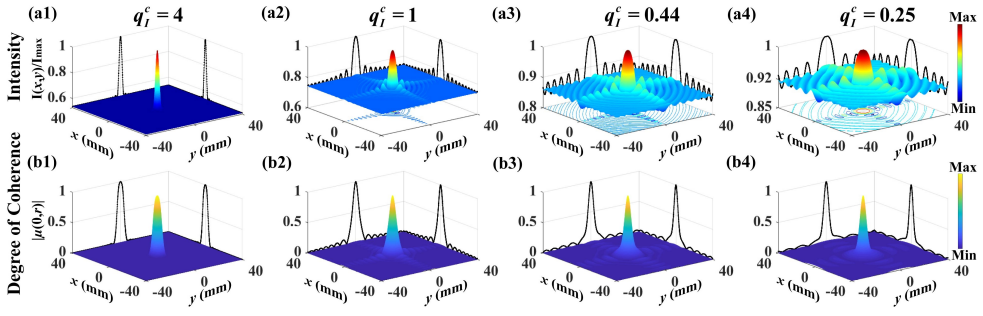

Fig. 1. The normalized intensity (top) and modulus of degree of coherence (bottom) distributions of a diffraction-free partially coherent Pearcey beams without truncation in the source plane. From left to right, the global coherence q_I^c decreases from 4 to 0.25. The coherent width σ_c is set to σ_c = 1mm.

peak of the intensity becomes wider, and the fluctuations arises around it; for the degree of coherence, the main central keeps almost invariant, but there will be slight oscillations around it. As demonstrated above, this beam possesses the ability to resist the optical diffraction.

To provide further insights, we consider the truncated version, and its evolution behaviors are shown in Fig. 2. The width of the truncated Gaussian profile is set to σ_0 = 10mm. The total propagation distance is 100m, spanning from the left plane to the right plane. The results vividly demonstrate both the intensity (left panel) and modulus of degree of coherence (right panel) hold almost invariant throughout the propagation.

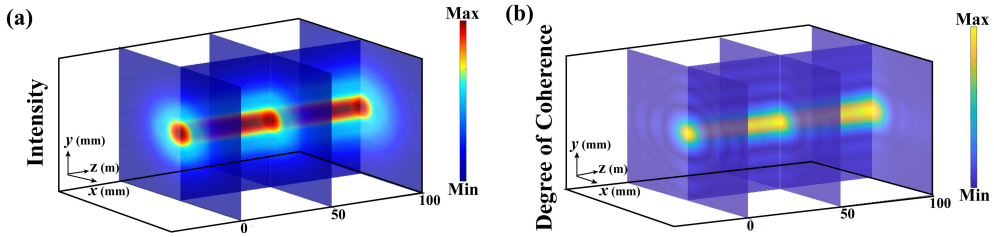

Fig. 2. The normalized intensity (left panel) and modulus of degree of coherence (right panel) of a truncated diffraction-free partially coherent Pearcey beams during propagation in free space. Each plot shows three planes corresponding to propagation distances at z=0, 50m and 100m. Other parameters are set as q_I^c = 1 and σ_c = 1mm.

To quantitatively describe the beam's ability to resist optical diffraction, we introduce the degree of similarity to evaluate the similarity between the intensity (or degree of coherence) distribution in the receiver plane and that in the source plane. The degree of similarity is defined as follows: [41]

$$DS(z) = \frac{\left[\iint \Omega(\mathbf{r}, z) \times \Omega_0(\mathbf{r}) d^2\mathbf{r}\right]^2}{\iint \Omega^2(\mathbf{r}, z)\, d^2\mathbf{r} \iint \Omega_0^2(\mathbf{r})\, d^2\mathbf{r}}, \tag{11}$$

where $\Omega(\mathbf{r}, z)$ stands for the intensity or modulus of degree of coherence profile at the propagation distance z, and $\Omega_0(\mathbf{r})$ represents for the one in the source plane. Its value falls within the interval [0, 1], and the bigger value demonstrates more power to be immune to the optical diffraction.

In Fig. 3, we plot the degree of similarity curves for intensity (blue curves) and modulus of degree of coherence (red curves). It can be observed that while the curves slightly decrease with propagation distance, the degree of similarity remains around 0.98 at a propagation distance of z =

Optics EXPRESS

100m, confirming the beam's strong ability to resist optical diffraction. Furthermore, we examine the effect of the global coherence q_I^c, the only varying parameter, on the degree of similarity of both intensity and degree of coherence. The results illustrate both remain largely unaffected by this parameter, except for minor variations in the degree of coherence (mainly due to the susceptibility of its fine structure to disruption). This suggests that the constructed beam, even with low coherence, still retains a remarkable anti-diffraction capability. This effectively resolves the traditional dilemma, where lower beam coherence typically results in greater diffraction and more pronounced light field distortion.

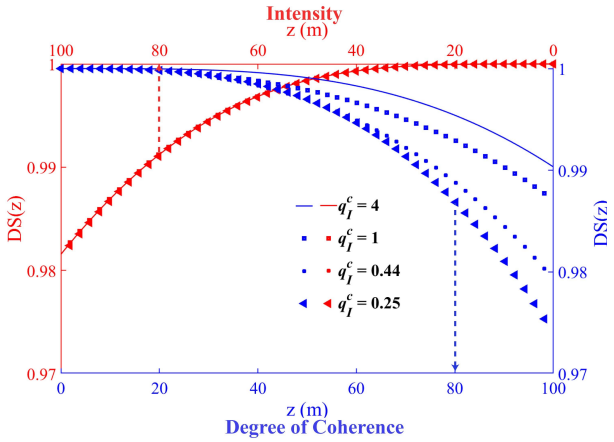

Fig. 3. The degree of similarity of intensity (blue curves) and degree of coherence (red curves) of a truncated diffraction-free partially coherent Pearcey beam during propagation in free space. Other parameters are set as σ_c = 1mm and σ_0 = 10mm.

4. Experimental verification

In this section, we experimentally realize the diffraction-free partially coherent Pearcey beams, with the help of the incoherent superposition of pseudo-modes approach. The optical setup is depicted by Fig. 4. The beam, emitted from He-Ne laser with the wavelength λ = 632.8nm, passes through a half-wave plate and is expanded by a beam expander. We adjust the orientation of the half-wave plate to align the polarization of the outgoing beam horizontally, as required for optimal response from the SLM. After passing through a beam splitter, the beam illuminates the phase-only spatial light modulator (SLM). We utilize the complex amplitude modulation encoding algorithm [42] to design the gratings loaded onto the SLM, enabling customization of the specified pseudo-mode as described by Eq. (3). The SLM phase corresponding to the electric field to be encoded is represented

$$\phi_{SLM} = B \sin\left\{\mathrm{Arg}\left[A\left(\mathbf{k}_{mn}, \mathbf{r}\right)\right] + 2\pi f_x x\right\}, \tag{12}$$

where the amplitude B is achieved through numerical inversion: $J_1(B) = |A(\mathbf{k}_{mn}, \mathbf{r})|$, where J_1 indicates a Bessel function of the first kind and first order; "Arg" represents taking the phase of a function. f_x stands for the grating frequency. The beam, after being reflected by the SLM and the beam splitter, passes through a modified 4f optical imaging system composing of two identical lenses and an iris (as shown in Fig. 4(a)). The iris, positioned in the frequency plane, is used to elect the positive or negative first-order diffraction beam. The desired pseudo-mode is captured by a CCD camera. We refresh the gratings on the SLM to achieve a large number of different modes (as depicted in Fig. 4(b)). These modes are then incoherently superposed to reconstruct

Optics EXPRESS

the diffraction-free partially coherent Pearcey beam. In our experiment, the relevant parameters are set as f=250mm, σ_I = 1mm, σ_c = 1mm and the total number of modes is 3600. In our experiment, the truncation function arises primarily from the limited size of the SLM (15.36 × 9.60 mm). Further, it can be inferred from Eqs. (2), (3), (9), and (10), all beam parameters, including beam width and coherence width, are determined by the pseudo-modes themselves. The partially coherent Pearcey beams we constructed in the experiment are very stable, because we employed the well-developed complex amplitude modulation encoding technique and our experimental setup is very simple. Additionally, all beam parameters can be preset during the hologram preparation process.

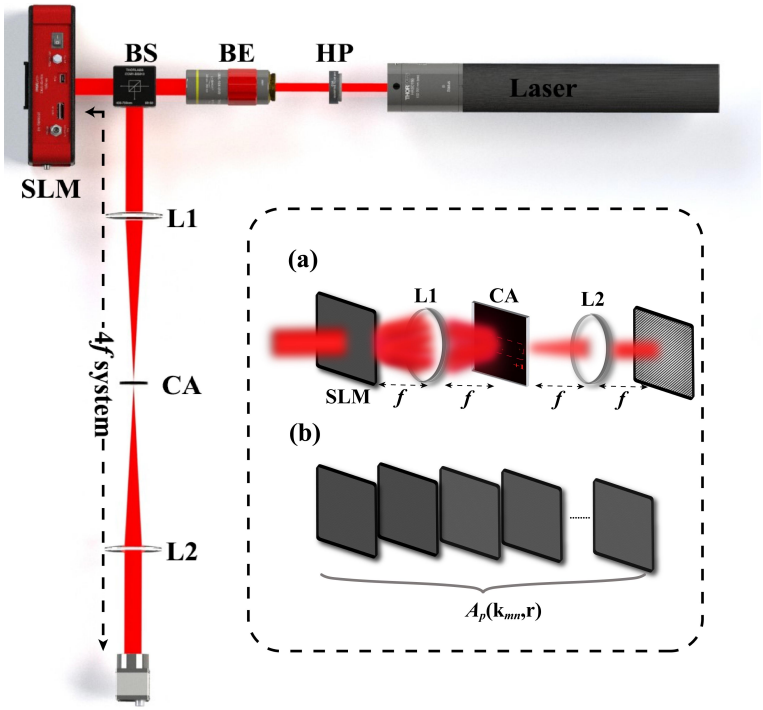

Fig. 4. The optical setup for construction of the diffraction-free partially coherent Pearcey beam. (a) The modified 4f imaging system composing of two identical lenses and an iris is used to select the desired pseudo-mode, lying the positive or negative first-order diffraction beam. (b) The gratings loading on the SLM are refreshed to generate a large number of different pseudo-modes. HP: half-wave plate; BE: beam expander; BS: beam splitter; SLM: phase-only spatial light modulator; L1, L2: lenses; CA: circular aperture.

First, we experimentally construct diffraction-free partially coherent Pearcey beams with the different value of the parameter q_I^c in the source plane, and the corresponding results are presented in Fig. 5. The theoretical results, experimental results, and the data fitting of both are shown in the first, second, and third rows of Fig. 5, respectively. The experimental results are in good agreement with the theoretical ones, demonstrating the feasibility of our proposal. The slight difference arises from the limited pixel size of the SLM (8 μm in our laboratory), which results in imperfect reconstruction of certain pseudo modes with fine structures. In addition, we further investigate the propagation behavior of the beam in free space experimentally. The relevant results are displayed in Fig. 6. One finds that the intensity does not change as the beam propagates. The experimental outcomes align well with the theoretical predictions, confirming our constructed partially coherent beams have a strong ability to resist optical diffraction.

Optics EXPRESS

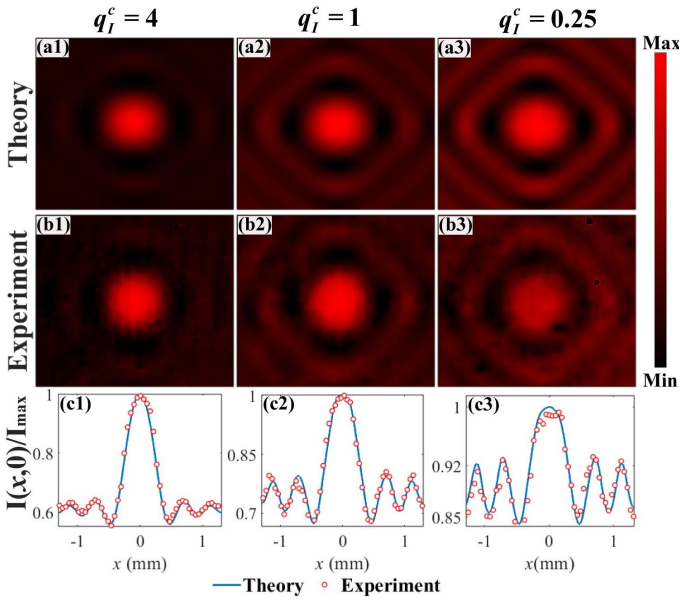

Fig. 5. The theoretical and experimental results of the intensity profiles of diffraction-free partially coherent Pearcey beams in the source plane with different value of the global coherence q_I^c. From left to right, q_I^c is respectively set to 4, 1, and 0.25. Other parameter is set as σ_c = 1mm.

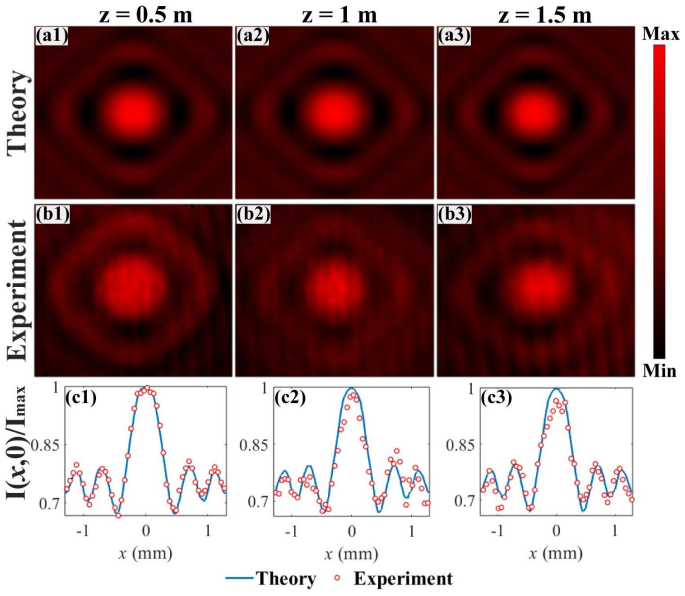

Fig. 6. The theoretical and experimental results of the intensity profiles of the diffraction-free partially coherent Pearcey beams during propagation in free space. From left to right, the propagation distances z are respectively set as 0.5m, 1m, and 1.5m. Other parameters are set to q_I^c =1 and σ_c = 1mm.

Optics EXPRESS

5. Conclusion

In this paper, we theoretically propose and experimentally advance the customization of diffraction-free partially coherent Pearcey beams, through the incoherent superposition of pseudo-modes. Although it takes a longer time to achieve beam synthesis, we can accelerate the process by using an SLM or digital micromirror device with a high refresh rate. The intensity and degree of coherence of such beams hold invariant during propagation. Even in practical scenarios, the truncated version still retains the prominent ability to resist optical diffraction. These beams naturally possess two significant advantages: low coherence and diffraction-free propagation. The low coherence ensures the beam's robustness in adverse environment, while the diffraction-free nature allows the use of certain degree of freedom, such as the intensity and degree of coherence, as the information carrier for long-distance information transfer. Consequently, diffraction-free partially coherent Pearcey beams hold great potential for applications in optical communication, information transfer, optical imaging particularly in the adverse environment.

Funding. National Key Research and Development Program of China (2022YFA1404800); National Natural Science Foundation of China (12374311, 12192254, 92250304, W2441005); Taishan Scholar Foundation of Shandong Province (tsqn202312163); Qingchuang Science and Technology Plan of Shandong Province (2022KJ246); China Postdoctoral Science Foundation (2022T150392); Natural Science Foundation of Shandong Province (ZR2023YQ006, ZR2024QA012, ZR2024QA216); Natural Sciences and Engineering Research Council of Canada (RGPIN-2018-05497).

Disclosures. The authors declare no conflicts of interest.

Data availability. Data underlying the results presented in this paper are not publicly available at this time but may be obtained from the authors upon reasonable request.

References

1. L. Mandel and E. Wolf, *Optical Coherence and Quantum Optics* (Cambridge University Press, 1995).
2. Z. Shi, Z. Wan, Z. Zhan, *et al.*, "Super-resolution orbital angular momentum holography," Nat. Commun. **14**(1), 1869 (2023).
3. J. N. Clark, X. Huang, R. Harder, *et al.*, "High-resolution three-dimensional partially coherent diffraction imaging," Nat. Commun. **3**(1), 993 (2012).
4. B. Redding, M. A. Choma, and H. Cao, "Speckle-free laser imaging using random laser illumination," Nat. Photonics **6**(6), 355–359 (2012).
5. B. Dong, F. B. Plückelmann, L. Meyer, *et al.*, "Partial coherence enhances parallelized photonic computing," Nature **632**(8023), 55–62 (2024).
6. T. Shirai, A. Dogariu, and E. Wolf, "Mode analysis of spreading of partially coherent beams propagating through atmospheric turbulence," J. Opt. Soc. Am. A **20**(6), 1094 (2003).
7. Z. Xu, X. Liu, Y. Cai, *et al.*, "Structurally stable beams in the turbulent atmosphere: dark and antidark beams on incoherent background [Invited]," J. Opt. Soc. Am. A **39**(12), C51 (2022).
8. X. Li, Y. Wang, X. Liu, *et al.*, "Deep learning and random light structuring ensure robust free-space communications," Appl. Phys. Lett. **124**(21), 214103 (2024).
9. X. Liu, S. A. Ponomarenko, F. Wang, *et al.*, "Incoherent mode division multiplexing for high-security information encryption," arXiv (2023).
10. Y. Liu, Y. Chen, F. Wang, *et al.*, "Robust far-field imaging by spatial coherence engineering," Opto-Electron. Adv. **4**(12), 210027 (2021).
11. F. Wang, C. Liang, Y. Yuan, *et al.*, "Generalized multi-Gaussian correlated Schell-model beam: from theory to experiment," Opt. Express **22**, 23456–23464 (2014).
12. O. Korotkova, *Random Light Beams Theory and Applications* (CRC, 2014).
13. C. Liang, G. Wu, F. Wang, *et al.*, "Overcoming the classical Rayleigh diffraction limit by controlling two-point correlations of partially coherent light sources," Opt. Express **25**(23), 28352 (2017).
14. X. Liu, C. Liang, Y. Cai, *et al.*, "Axial correlation revivals and number factorization with structured random waves," Phys. Rev. Appl. **20**(2), L021004 (2023).
15. T. Cao, X. Liu, Q. Chen, *et al.*, "Prime number factorization and degree of coherence of speckled light beams," Opt. Lett. **49**(18), 5232 (2024).
16. D. Peng, Z. Huang, Y. Liu, *et al.*, "Optical coherence encryption with structured random light," PhotoniX **2**(1), 6 (2021).
17. F. Wang, X. Liu, Y. Yuan, *et al.*, "Experimental generation of partially coherent beams with different complex degrees of coherence," Opt. Lett. **38**, 1814–1816 (2013).
18. L. Liu, W. Liu, F. Wang, *et al.*, "Spatial coherence manipulation on the disorder-engineered statistical photonic platform," Nano Lett. **22**(15), 6342–6349 (2022).

Optics EXPRESS

19. L. Liu, W. Liu, F. Wang, *et al.*, "Ultra-robust informational metasurfaces based on spatial coherence structures engineering," Light: Sci. Appl. **13**(1), 131 (2024).
20. Y. Cai, Y. Chen, and F. Wang, "Generation and propagation of partially coherent beams with non-conventional correlation functions: a review," J. Opt. Soc. Am. A **31**(9), 2083 (2014).
21. Y. Chen, F. Wang, and Y. Cai, "Partially coherent light beam shaping via complex spatial coherence structure engineering," Adv. Phys.-X **7**, 2009742 (2022).
22. J. Yu, X. Zhu, F. Wang, *et al.*, "Research progress on manipulating spatial coherence structure of light beam and its applications," Prog. Quant. Electron. **91-92**, 100486 (2023).
23. Y. Liu, Z. Dong, Y. Zhu, *et al.*, "Three-channel robust optical encryption via engineering coherence Stokes vector of partially coherent light," PhotoniX **5**(1), 8 (2024).
24. X. Lu, Z. Wang, Q. Zhan, *et al.*, "Coherence entropy during propagation through complex media," Adv. Photonics **6**(04), 046002 (2024).
25. J. Durnin, "Exact solutions for nondiffracting beams. I. The scalar theory," J. Opt. Soc. Am. A **4**(4), 651 (1987).
26. J. Durnin, J. J. Miceli Jr., J. H. Eberly, *et al.*, "Eberly, Diffraction-free beams," Phys. Rev. Lett. **58**(15), 1499–1501 (1987).
27. Q. Chen, M. Hajati, X. Liu, *et al.*, "Experimental realization of Airy beams on incoherent background," Opt. Laser Technol. **169**, 110020 (2024).
28. T. Vettenburg, H. I. Dalgarno, J. Nylk, *et al.*, "Light-sheet microscopy using an airy beam," Nat. Methods **11**(5), 541–544 (2014).
29. D. Phillips, R. He, Q. Chen, *et al.*, "Non-diffractive computational ghost imaging," Opt. Express **24**(13), 14172 (2016).
30. J. Baumgartl, M. Mazilu, and K. Dholakia, "Optically mediated particle clearing using airy wavepackets," Nat. Photonics **2**(11), 675–678 (2008).
31. D. N. Naik, R. K. Singh, T. Ezawa, *et al.*, "Photon correlation holography," Opt. Express **19**(2), 1408 (2011).
32. J. Turunen, A. Vasara, and A. T. Friberg, "Propagation invariance and self-imaging in variable-coherence optics," J. Opt. Soc. Am. A **8**(2), 282 (1991).
33. S. A. Ponomarenko, W. Huang, and M. Cada, "Dark and antidark diffraction-free beams," Opt. Lett. **32**(17), 2508 (2007).
34. M. Hajati, V. Sieben, and S. A. Ponomarenko, "Airy beams on incoherent background," Opt. Lett. **46**(16), 3961 (2021).
35. A. S. Ostrovsky, J. Garcí-Garcí, C. Rickenstorff-Parrao, *et al.*, "Partially coherent diffraction-free vortex beams with a Bessel-mode structure," Opt. Lett. **42**(24), 5182 (2017).
36. Z. Pang and D. Zhao, "Partially coehrent dual and quad airy beams," Opt. Lett. **44**(19), 4889 (2019).
37. Z. Pang, X. Zhou, Z. Liu, *et al.*, "Partially coherent quasi-Airy beams with controllable acceleration," Phys. Rev. A **102**(6), 063519 (2020).
38. Y. Lumer, Y. Liang, R. Schley, *et al.*, "Incoherent self-accelerating beams," Optica **2**(10), 886 (2015).
39. X. Chen, D. Deng, J. Zhuang, *et al.*, "Focusing properties of circle Pearcey beams," Opt. Lett. **43**, 3626–3629 (2018).
40. X. Chen, D. Deng, G. Wang, *et al.*, "Abruptly autofocused and rotated circular chirp Pearcey Gaussian vortex beams," Opt. Lett. **44**, 955–958 (2019).
41. Z. Xu, X. Liu, Y. Chen, *et al.*, "Self-healing properties of Hermite-Gaussian correlated Schell-model beams," Opt. Express **28**, 2828–2837 (2020).
42. X. Liu, Y. E. Monfared, R. Pan, *et al.*, "Experimental realization of scalar and vector perfect Laguerre–Gaussian beams," Appl. Phys. Lett. **119**(2), 021105 (2021).

159.2.37.176 {ts '2025-01-14 11:52:10'}